Published in final edited form as:
*Nat Neurosci*. 2006 June ; 9(6): 807–815. doi:10.1038/nn1688.

# Distinct timing in the activity of cannabinoid-sensitive and cannabinoid-insensitive basket cells

**Lindsey L Glickfeld**[1] and **Massimo Scanziani**[1]

[1]Neuroscience Graduate Program and Neurobiology Section, Division of Biology, University of California San Diego, La Jolla, California, 92093, USA

## Abstract

Cannabinoids are powerful modulators of inhibition, yet the precise spike timing of cannabinoid receptor (CB1R)-expressing inhibitory neurons in relation to other neurons in the circuit is poorly understood. Here we found that the spike timing of CB1R-expressing basket cells, a major target for cannabinoids in the rat hippocampus, was distinct from the other main group of basket cells, the CB1R-negative. Despite receiving the same afferent inputs, the synaptic and biophysical properties of the two cell types were tuned to detect different features of activity. CB1R-negative basket cells responded reliably and immediately to subtle and repetitive excitation. In contrast, CB1R-positive basket cells responded later and did not follow repetitive activity, but were better suited to integrate the consecutive excitation of independent afferents. This temporal separation in the activity of the two basket cell types generated distinct epochs of somatic inhibition that were differentially affected by endocannabinoids.

Basket cells are a class of GABAergic interneurons that synapse specifically onto the somata of their targets[1]. From this advantageous location, basket cells can perform a variety of temporally precise operations, which include the synchronization of neural ensembles, the pacing of rhythmic activity and the control of spike timing and synaptic integration[2–7]. A substantial fraction of cannabinoid receptors (CB1R) in cortical areas are located on the synaptic terminals on one type of basket cell[8–11]. When exposed to endocannabinoids, as during depolarization of the postsynaptic pyramidal cell, CB1Rs inhibit GABA release, effectively reducing the magnitude of somatic inhibition onto that pyramidal cell[12–14]. Yet, despite the strategic position of basket cell terminals, the specific role of CB1R-positive basket cells, and therefore endocannabinoids, in controlling network activity is poorly understood[8].

The function of each type of GABAergic interneuron is determined by the interplay between the excitation it receives from its inputs, its intrinsic electrophysiological properties, and the inhibition it exerts on its targets. Individual interneuron types are preferentially recruited by the specific activity patterns of their inputs[15–19] and, owing to their distinct axonal projections[20], inhibit specific regions along the soma-todendritic axis of their targets. The participation of distinct classes of interneurons during complementary phases of hippocampal oscillations *in vivo* provides further evidence of the differential recruitment of



Correspondence should be addressed to M.S. (massimo@ucsd.edu).

Note: Supplementary information is available on the Nature Neuroscience website.

**COMPETING INTERESTS STATEMENT**

The authors declare that they have no competing financial interests.

cell types[21,22]. Here we found that CB1R-positive basket cells received weak and very transient excitation, which, however, they integrated over long time windows and across many afferents. This makes them ideally suited to detect the sequential activation of independent excitatory inputs. In contrast, CB1R-negative basket cells received stronger and more persistent excitation, which they integrated only over very narrow time windows, thereby faithfully reporting the timing of ongoing hippocampal activity. Because of their sensitivity to distinct activity patterns, CB1R-positive and -negative basket cells were recruited at different times. Hence, endocannabinoids regulate the inhibition resulting from global changes in activity while leaving the more precise inhibitory control intact.

## RESULTS

By simultaneously recording from basket cells (ascertained by *post-hoc* morphological analysis) and their pyramidal cell targets, we identified two types of unitary inhibitory connections: those that were suppressed by pyramidal cell depolarization (to 0 mV for 5 s; depolarization-induced suppression of inhibition (DSI)) and those that were not (Fig. 1a). The suppression could be blocked by the specific CB1R antagonist AM251 (5 μM; $n = 4$; Fig. 1b), and the antibody to CB1R colocalized with the axons of DSI-sensitive but not DSI-insensitive basket cells ($n = 5$ and 4, respectively; Fig. 1c). Therefore, we classified the two types of basket cells as CB1R-positive and CB1R-negative ($n = 28$ and 26; Fig. 1d–e). The two types of basket cells (Fig. 2a) clearly differed in their membrane time constants (CB1R-positive: 25.0 ± 1.8 ms; CB1R-negative: 10.2 ± 0.6 ms; $P < 0.0001$; $n = 18$ and 22; Fig. 2b) and input resistances (151.6 ± 12.0 MΩ; 64.5 ± 6.3 MΩ; $P < 0.0001$; $n = 22$ and 26; Fig. 2b). Further, they also had distinct patterns of spike frequency adaptation (CB1R-positive were adapting, adaptation coefficient = 0.33 ± 0.02; CB1R-negative were nonadapting, adaptation coefficient = 0.82 ± 0.02; $P < 0.0001$; $n = 24$ and 25; Fig. 2c), distinct unitary inhibitory postsynaptic current (uIPSC) rise times (0.90 ± 0.06 ms; 0.66 ± 0.06 ms; $P < 0.005$; $n = 26$ and 24; Fig. 2d) and distinct synaptic conduction delays (1.6 ± 0.1 ms; 0.7 ± 0.1 ms; $P < 0.0001$; $n = 27$ and 24; Fig. 2e), similar to interneurons expressing cholecystokinin and parvalbumin, respectively, in the dentate gyrus[23]. However, the uIPSCs that they evoked on their targets were indistinguishable in terms of peak conductance (1.2 ± 0.2 nS; 1.1 ± 0.2 nS; $P > 0.5$; $n = 28$ and 26; Fig. 2d), decay time constant (7.3 ± 0.6 ms; 6.7 ± 0.3 ms; $P > 0.3$; $n = 24$ and 23; Fig. 2d) and paired pulse ratio (0.79 ± 0.06; 0.71 ± 0.02; $P > 0.3$; $n = 21$ and 12; Fig. 2d).

In all subsequent experiments, every recording of a *post-hoc* morphologically identified basket cell began by establishing its cannabinoid sensitivity by finding a postsynaptically connected pyramidal cell and determining the magnitude of suppression of the uIPSC in response to pyramidal cell depolarization.

### Target-specific excitation of basket cells

The similar anatomical distribution (Fig. 2a; see Supplementary Fig. 1 online for individual reconstructions) and physiological properties (Fig. 2d) of synapses formed by CB1R-positive and -negative basket cells onto pyramidal cells suggest that the two cell types inhibit their targets in a similar manner. However, CB1R-positive and -negative basket cells may be differently excited by their afferents. To test this possibility, we compared the amplitude and dynamics of excitatory postsynaptic currents (EPSCs) evoked by afferent stimulation onto CB1R-positive and -negative basket cells.

The amplitude of EPSCs evoked with an extracellular stimulation electrode may vary strongly between experiments depending on stimulation intensity, the exact position of the stimulation electrode, electrical properties of the stimulation electrode and quality of the stimulated tissue, all parameters that will affect the number of stimulated fibers. These

sources of variability preclude meaningful comparison of EPSC amplitudes recorded during different experiments. To make this comparison, we used a reliable readout of the stimulation conditions during each experiment: the simultaneously recorded, postsynaptic pyramidal cell. By normalizing the amplitude of the evoked EPSC recorded in a basket cell with the EPSC recorded simultaneously in the pyramidal cell voltage-clamped at the same potential, we were able to control for the sources of variability mentioned above and compare the relative amount of excitation received by CB1R-positive and -negative basket cells across experiments.

We stimulated the three major excitatory pathways in area CA1, the perforant path, the Schaffer collaterals and the CA1 pyramidal cell axons, by placing stimulation electrodes in the stratum lacunosum moleculare, the stratum radiatum and the alveus, respectively. These three pathways converged onto individual CB1R-positive and -negative basket cells (Fig. 3a), suggesting that each basket cell can potentially participate in both feedforward and feedback inhibition.

Despite the fact that CB1R-positive and -negative basket cells were excited by the same afferents, the amplitude and short-term plasticity of evoked EPSCs were markedly different between the two cell types. Stimulation of the Schaffer collaterals (in the presence of the $GABA_A$ receptor antagonist gabazine or at the IPSC reversal potential to isolate glutamatergic transmission) evoked much larger EPSCs in CB1R-negative basket cells than in the simultaneously recorded postsynaptic pyramidal cells. The peak amplitude of Schaffer collateral–mediated EPSCs was 8.15 ± 1.50 times larger onto CB1R-negative basket cells as compared to their pyramidal cell targets ($P < 0.005$; $n = 16$ pairs; Fig. 3b). In contrast, when recording from CB1R-positive basket cells and their postsynaptic pyramidal cells, Schaffer collateral stimulation elicited EPSCs that were of similar amplitude (1.09 ± 0.36 times larger in CB1R-positive basket cells; $P > 0.05$; $n = 16$ pairs; Fig. 3b). Comparison of the normalized EPSCs recorded in the CB1R-positive and -negative basket cells indicated that the stimulation of Schaffer collaterals evoked EPSCs that were 7.5 times larger in CB1R-negative as compared to -positive basket cells ($P < 0.0001$).

It is unlikely that this difference in amplitude was due to a stronger postsynaptic attenuation of Schaffer collateral–evoked EPSCs in CB1R-positive as compared to -negative basket cells, because the rise times of the evoked EPSCs were indistinguishable (10–90% EPSC rise time; CB1R-positive = 1.16 ± 0.14 ms; CB1R-negative = 1.02 ± 0.11 ms; $P > 0.4$; $n =$ 11 and 18).

Short-term plasticity of EPSCs evoked by repetitive Schaffer collateral stimulation was also different between CB1R-positive and -negative basket cells. In fact, EPSCs depressed significantly more in CB1R-positive as compared to -negative basket cells at all frequencies tested ($P < 0.005$; Fig. 4a and Table 1). Hence, CB1R-negative basket cells receive stronger and more persistent excitation as compared to CB1R-positive basket cells, suggesting that they are the primary mediators of feedforward inhibition to CA1 pyramidal cells.

We next tested whether the differences in the magnitude and dynamics of excitation between the two types of basket cells is specific to Schaffer collateral inputs or whether it also extends to the two other major excitatory pathways: the perforant path and the CA1 pyramidal cell axon collaterals. As with the Schaffer collateral input, stimulation of the perforant path evoked EPSCs that were larger ($EPSC_{CB1R+}/EPSC_{Pyr}$ = 1.21 ± 0.30; $EPSC_{CB1R-}/EPSC_{Pyr}$ = 3.35 ± 0.95; $P < 0.05$; $n = 7$ and 5; Fig. 3b) and less depressing $P <$ 0.005 (Fig. 4b and Table 1) on CB1R-negative than CB1R-positive basket cells.

Similarly, stimulation of the alveus elicited EPSCs that depressed significantly ($P < 0.0005$) more in CB1R-positive as compared to CB1R-negative basket cells (Fig. 4c and Table 1).

As CA1 pyramidal cells form few, if any, recurrent synapses with other CA1 pyramidal cells[24], no reference EPSC could be recorded in response to alveus stimulation in the postsynaptic pyramidal cells. This prevented the comparison of the relative magnitude of excitation produced by CA1 pyramidal cells onto the two basket cell types. These data clearly show that CB1R-positive basket cells receive weaker and more depressing excitation from their major excitatory inputs than CB1R-negative basket cells.

## Transient recruitment of CB1R-positive basket cells

The strongly depressing EPSCs evoked onto CB1R-positive basket cells suggests that their recruitment during ongoing hippocampal activity may be very transient as compared to that of CB1R-negative basket cells. To test this possibility, we recorded from basket cells in the whole-cell, current-clamp configuration and repetitively stimulated the alveus (5 stimuli at 20 Hz) at an intensity that was at threshold to trigger an action potential in the basket cell after the first stimulus in the train. The probability of the alvear input triggering an action potential in CB1R-positive basket cells decreased sharply with repetitive stimulation (from 57 ± 9% after the first stimulus to 0 after the fifth stimulus; $P < 0.001$; $n = 4$; Fig. 5a). In contrast, in CB1R-negative basket cells, the spiking probability remained more sustained during the train (from 69 ± 4% after the first stimulus to 32 ± 16% after the fifth stimulus; $P > 0.05$; $n = 4$; Fig. 5a).

The observed differential activation of the two basket cell types by the alvear input predicts that CB1R-positive basket cells will only transiently contribute to disynaptic inhibition of pyramidal cells during repetitive stimulation of the alveus. We tested this hypothesis by evoking disynaptic inhibitory postsynaptic currents (IPSCs) in pyramidal cells via alveus stimulation. The disynaptic origin of the IPSC was confirmed by the fact that it was abolished by the glutamate receptor antagonist 2,3-dihydroxy-6-nitro-7-sulfamoyl-benzo(f) quinoxaline (NBQX, 10 μM; Fig. 5b). To quantify the relative contribution of CB1R-positive basket cells to the disynaptic IPSC, we briefly depolarized the pyramidal cell, thereby suppressing GABA release from CB1R-positive basket cells via endocannabinoid signaling. The contribution of CB1R-positive basket cells to the disynaptic IPSC recorded in pyramidal cells was essentially restricted to the very first stimulus in a series (DSI first stimulus = 30 ± 9%; DSI fifth stimulus = −3 ± 8%; $P < 0.05$; $n = 3$; Fig. 5b). In contrast, interneurons mediating the cannabinoid-insensitive component (which may include basket, axo-axonic and bistratified cells) seem to be recruited repetitively during the stimulus train. The transient contribution by CB1R-positive basket cells was not due to the depression of GABA release from their terminals because direct stimulation of the GABAergic axons (in the presence of NBQX) elicited monosynaptic IPSCs whose endocannabinoid-sensitive component remained unaltered during the entire train of stimuli (DSI first stimulus = 37 ± 8%; DSI fifth stimulus = 36 ± 7%; $P > 0.4$; $n = 3$; Fig. 5c, d). Hence, these data demonstrate that whereas repetitive activation of excitatory afferents only transiently recruits CB1R-positive basket cells, CB1R-negative cells are able to spike throughout a train of stimuli.

## CB1R-positive basket cells are integrators

As CB1R-positive basket cells respond poorly to the repetitive activation of a single pathway, they may be preferentially recruited when two or more independent pathways are active in succession. Because the ability of a neuron to integrate independent inputs depends critically on the amount of inhibition it receives[5,25], we compared the magnitude of disynaptic inhibition onto CB1R-positive and -negative basket cells. For this, we stimulated excitatory afferents and used the disynaptic IPSC recorded in pyramidal cells as a reference in the same manner as we did when comparing the amplitude of EPSCs (Fig. 6a).

CB1R-negative basket cells received larger disynaptic IPSCs as compared to pyramidal cells in response to both Schaffer collateral stimulation (CB1R-negative = 361.5 ± 83.0 pA; Pyr = 166.4 ± 21.4 pA; $P$ <0.05; $n$ = 13; Fig. 6b) and alveus stimulation (CB1R-negative = 206.2 ± 31.4 pA; Pyr = 95.9 ± 22.1 pA; $P$ < 0.05; $n$ = 12; Fig. 6b). The onset of the disynaptic IPSC (10% of peak amplitude) recorded in CB1R-negative basket cells occurred with a delay of 1.64 ± 0.11 ms ($n$ = 25) with respect to the onset of the monosynaptic EPSC, consistent with its disynaptic origin[5]. In contrast, CB1R-positive basket cells received a much smaller disynaptic IPSC as compared to pyramidal cells in response to stimulation of either pathway (Schaffer collaterals: CB1R-positive = 17.1 ± 4.9 pA, Pyr = 242.8 ± 50.3 pA, $P$ < 0.005, $n$ = 12; Alveus: CB1R-positive = 22.8 ± 6.7 pA, Pyr = 107.5 ± 29.4 pA, $P$ < 0.05, $n$ = 12; Fig. 6b). The onset of the small disynaptic IPSC occurred with a delay of 2.89 ± 0.35 ms ($n$ = 13) with respect to the onset of the monosynaptic EPSC.

We next tested whether this marked difference in the amount of inhibition received by the two basket cell types influences their ability to integrate consecutive inputs. We recorded from basket cells and applied a stimulus to the Schaffer collaterals, which was followed, with a variable delay, by a stimulus to the alveus. The lack of disynaptic inhibition enabled CB1R-positive basket cells to summate EPSPs originating from the two distinct afferents over much longer time windows than CB1R-negative cells (summation at 10 ms interval: CB1R-positive = 0.66 ± 0.07, CB1R-negative = 0.13 ± 0.06, $P$ < 0.0001, $n$ = 7 and 10; Fig. 6c).

The very brief integration window of CB1R-negative basket cells was, at least in part, due to the presence of inhibition. Accordingly, the application of the $GABA_A$ receptor antagonist gabazine increased the integration window of CB1R-negative basket cells to values comparable with their membrane time constant (summation at 10 ms interval: CB1R-negative control =0.13 ± 0.06, gabazine = 0.61 ± 0.05, $P$ < 0.0005, $n$ = 10 and 5; Fig. 6d).

We next determined whether these two different integration windows influence summation within physiologically relevant intervals. When Schaffer collateral stimulation was above threshold to trigger action potentials in CA1 pyramidal cells, two consecutive EPSCs were recorded in basket cells: the first was due to direct Schaffer collateral excitation (feedforward EPSC; Fig. 7a) and the second was due to feedback excitation through the recurrent axon collaterals of CA1 pyramidal cells (feedback EPSC; Fig. 7a). The amplitude of the population spike (simultaneously recorded in the CA1 pyramidal cell layer) increased in a sigmoidal manner with the feedforward EPSC amplitude, as expected[26,27]. In contrast, the amplitude of the late, feedback EPSC increased linearly with the amplitude of the population spike[27], indicating that this second EPSC was indeed triggered by the spiking of CA1 pyramidal cells (data not shown). The average delay between the onset of the feedforward and feedback EPSC varied between 3 ms and 5 ms, depending on stimulation intensity (delay at threshold stimulation intensity for feedback EPSC = 4.94 ± 0.73 ms, $n$ = 7; delay at maximal stimulation intensity = 3.19 ± 0.25 ms; range = 2.1–4 ms, $n$ = 7; Fig. 7a and shaded region in Fig. 7b). Notably, this interval was larger than the integration window of CB1R-negative basket cells but shorter than the integration window of CB1R-positive basket cells. Our data thus indicate that by operating as precise coincidence detectors, CB1R-negative basket cells can process the feedforward and the immediately following feedback excitation as two separate events. In contrast, the succession of feedforward and feedback EPSPs will summate within the broad integration window of CB1R-positive basket cells.

## Temporal separation in the recruitment of basket cells

The above results suggest that CB1R-negative basket cells will spike earlier than CB1R-positive basket cells in response to Schaffer collateral stimulation because the latter may integrate the succession of feedforward and feedback EPSPs before reaching threshold.

Furthermore, if CB1R-positive basket cells preferentially fire in response to the summation of feedforward and feedback EPSPs, they should contribute more to the feedback inhibition of CA1 pyramidal cells than to feedforward inhibition. We tested these two possibilities by first comparing the spike timing of the two basket cell types in response to Schaffer collateral stimulation and second by determining the relative contribution of CB1R-positive basket cells to the feedforward and feedback inhibition of CA1 pyramidal cells.

When stimulating Schaffer collaterals at the threshold for spike generation (CB1R-positive: spiking probability = 40 ± 4%, membrane potential before EPSP onset = −57.7 ± 1.9 mV; CB1R-negative: spiking probability = 50 ± 7%, membrane potential before EPSP onset = −57.7 ± 0.8 mV; $P > 0.4$ for spiking probability, $P > 0.9$ for membrane potential; $n = 4$ and 9; Fig. 7c, d), the action potential occurred later in CB1R-positive basket cells than in CB1R-negative cells (delay from onset of EPSP: CB1R-positive = 5.1 ± 0.4 ms, CB1R-negative = 1.9 ± 0.1 ms, $P < 0.0001$, $n = 4$ and 9; jitter of action potentials: CB1R-positive = 0.37 ± 0.02, CB1R-negative = 0.29 ± 0.05 ms, $P > 0.3$, $n = 4$ and 9; Fig. 7c, d). Furthermore, in CB1R-positive basket cells, the response triggered by Schaffer collateral stimulation showed a biphasic rising phase, consistent with the integration of the feedforward-feedback EPSP sequence (Fig. 7d).

We next recorded from a CA1 pyramidal cell and stimulated the Schaffer collaterals to evoke feedforward and feedback inhibition. At low stimulation intensities, only feedforward inhibition could be recorded in pyramidal cells (Fig. 7e, blue trace). Increasing the stimulation intensity in order to trigger action potentials in a fraction of the CA1 pyramidal cell population resulted in the appearance a feedback IPSC (Fig. 7e, black trace), due to the recruitment of interneurons by CA1 pyramidal cells (as in the previous experiments: Fig. 7a, c).

To test whether CB1R-positive basket cells preferentially contribute to this later, feedback IPSC, we depolarized the pyramidal cell to suppress their GABA release via endocannabinoid signaling. Indeed, whereas CB1R-positive basket cells only weakly contributed to feedforward inhibition, they were responsible for the majority of feedback inhibition (percent suppression: feedforward = 6 ± 6%, feedback = 67 ± 14%, $n = 5$, $P < 0.05$; Fig. 7f).

Our data demonstrate that despite receiving the same excitatory afferents, CB1R-positive and -negative basket cells are recruited at different times (for schematic see Supplementary Fig. 2 online).

## DISCUSSION

The activity of CB1Rs modulates mood, perception and behavior[28]. A large fraction of these receptors in the cortex are localized to the presynaptic terminals of a specific population of basket cells, where they inhibit GABA release[2,10,11]. In the hippocampus, the two major populations of basket cells can be discriminated according to the selective expression of cholecystokinin (CCK) and parvalbumin, which correlate well with presence or absence of CB1Rs, respectively[10,11]. We found that CB1R-positive basket cells were recruited by the sequential activation of independent excitatory inputs, making them ideally suited to detect transitions in global activity. This pattern of activation was distinct from that necessary to recruit the other major group, CB1R-negative basket cells, resulting in a clear temporal separation in the activity of the two populations.

CB1R-positive and -negative basket cells were found to be embedded in the same network and received convergent inputs from the same main excitatory pathways. Thus, the temporal segregation in their activity, as apparent in the preferential participation of the two cell types

in feedforward or feedback inhibition, could not simply be explained by the connectivity. Rather, it was the magnitude and dynamics of excitation, the amount of disynaptic inhibition and the membrane time constant that determined their specific activity pattern.

On average, evoked EPSCs onto CB1R-negative basket cells were substantially larger than those onto CB1R-positive cells, independent of whether they originated from Schaffer collaterals or the perforant path, the two major excitatory afferents to the hippocampal CA1 region. This finding is consistent with anatomical data indicating that parvalbumin basket cells receive more excitatory synapses than CCK basket cells[29,30]. Differences in quantal amplitude, release probabilities and the number of release sites per axonal input may further contribute to the difference in EPSC amplitude between the two types of basket cells and will be addressed in the future. It should be mentioned that the difference in EPSC amplitude might not result in a correspondingly large difference in EPSP amplitude given the lower input resistance of CB1R-negative basket cells.

Stimulus trains over a broad range of frequencies (10–50 Hz) were more depressing onto CB1R-positive than -negative basket cells. This held true for each of the three major excitatory inputs converging on the two types of basket cells: the Schaffer collaterals, perforant path and CA1 pyramidal cell axons. The depression of excitatory inputs onto CB1R-positive basket cells could be due to a presynaptic decrease in the probabilities of transmitter release or to a postsynaptic desensitization of the receptors for released glutamate. The coefficient of variation of EPSC amplitude increased during the course of the stimulus train (first pulse = 0.19 ± 0.02, fifth pulse = 0.44 ± 0.06, $n = 9$, $P < 0.005$), suggesting at least some presynaptic contribution to the depression[31].

Anatomical data demonstrate that CCK basket cells receive more GABAergic synapses than parvalbumin basket cells[29,30]. In contrast, we found that whereas CB1R-negative basket cells were strongly inhibited, CB1R-positive basket cells received almost no inhibition. This apparent discrepancy could be explained by the presence of two interneuron subnetworks in which CB1R-positive and -negative interneurons preferentially target cells in their own class[7,32–35]. Given the stronger excitation received by the CB1R-negative basket cells, the afferent stimulation used in this study was likely to favor the activation of the CB1R-negative subnetwork.

The strong inhibition received by CB1R-negative basket cells, in conjuction with a fast membrane time constant, generates a narrow integration time window. This enabled CB1R-negative basket cells to discriminate inputs separated by as little as 3 ms. On the other hand, the weak inhibition and long membrane time constant of CB1R-positive basket cells enabled them to summate activity over longer intervals. Furthermore, because of the marked depression of their excitatory inputs, CB1R-positive basket cells were less likely to respond to the repetitive activation of a given set of inputs but were well suited to integrate sequential activity of independent inputs. In behaviorally relevant situations, consecutive activation of independent feed-forward excitatory afferents impinging on a hippocampal CB1R-positive basket cell in CA1 may occur when the movement of an animal in space triggers the sequential activation of CA3 pyramidal cells with different place fields.

An alternate situation involving the consecutive activity of independent pathway was explored here and results from the convergence of Schaffer collaterals and CA1 pyramidal cell axons onto individual basket cells. Our data showed that an evoked sequence of feedforward and feedback EPSPs occurred with the optimal interval to be treated as separate events in CB1R-negative basket cells while they will be integrated by CB1R-positive basket cells. The strong excitation of CB1-negative basket cells by Schaffer collaterals caused them to fire in response to the first event in the sequence and hence to provide feedforward

inhibition to their targets. In contrast, the weaker excitation received by CB1R-positive basket cells required the summation of both EPSPs in the sequence to trigger a spike. Hence CB1R-positive basket cells preferentially contributed to feedback inhibition, rendering this component exquisitely sensitive to endocannabinoids. Feedback inhibitory loops are believed to have an important role in the generation of rhythmic activity[36]. Specifically in the hippocampus, perisomatically targeting interneurons have been shown to entrain hippocampal gamma oscillations through feedback inhibition[2,37]. The contribution of CB1R-positive basket cells to feedback inhibition suggests that these neurons may participate in the modulation of the hippocampal gamma rhythm, a hypothesis supported by recent experimental observations[38].

By detecting distinct features of hippocampal activity, CB1R-positive and -negative basket cells were recruited at different times. The precise time of their recruitment may depend on the spatiotemporal activity pattern of their inputs, on the specific phase of a hippocampal oscillation or, more generally, on the behavioral state of the animal. Under specific behavioral conditions, such as exploration or attention, release of neuromodulators may alter the relative excitability of the two basket cells through selective receptor expression[8,39]. Thus, it is likely that cannabinoids will differentially affect the hippocampal network activity according to the prevailing behavioral state.

## METHODS

### Slice preparation and solutions

Hippocampal slices (400 μm) were prepared from 4- to 6-week-old male Wistar rats and incubated for 1 h in an interface chamber at 34 °C in artificial cerebrospinal fluid (ACSF) containing 119 mM NaCl, 2.5 mM KCl, 1.3 mM $NaH_2PO_4$, 1.3 mM $MgCl_2$, 2.5 mM $CaCl_2$, 26 mM $NaHCO_3$ and 11 mM glucose (equilibrated with 95% $O_2$ and 5% $CO_2$). The slices were kept at room temperature before being placed in a submerged chamber for recordings at 32–34 °C in the presence of the $GABA_B$ receptor antagonist CGP54626 (1 μM) and the NMDA receptor antagonist RS-CPP (25 μM). Whole-cell recordings were performed with patch pipettes (2–4 M) filled with 150 mM potassium gluconate, 1.5 mM $MgCl_2$, 5 mM HEPES buffer, 1.1 mM EGTA and10 mM phosphocreatine (pH = 7.25; 280–290 mOsm); biocytin (0.2%) and 2 mM Mg-ATP were added for interneurons. The drugs used were NBQX, SR95531 (‘gabazine’), CGP54626, R-(−)-3-(2-carboxypiper-azine-4-yl)-propyl-1-phosphonic acid (RS-CPP) and AM-251 (Tocris Cook-son). All experiments were conducted in accordance with the animal use guidelines set out by the University of California, San Diego.

### Electrophysiology and stimulation

Data were recorded with Multiclamp 700B and Axopatch 200A amplifiers (digitization 10 kHz). Voltage measurements were not corrected for the experimentally determined junction potential (−12 mV). Interneurons within 150 μm of the stratum pyramidale (in the strata pyrimidale, oriens and radiatum) were visually identified using infrared differential interference contrast (DIC) videomicroscopy. The spiking pattern of interneurons was determined immediately after achieving whole-cell con-figuration by a series of depolarizing step current injections (100–500 ms). The adaptation coefficient was determined by dividing the steady state spike frequency (average of the last 100 ms of the step depolarization) by the initial instantaneous frequency. Stimulation (100 μs) was performed using steel monopolar electrodes (FHC). One radial cut was made to separate the CA3 and CA1 regions, and a second radial cut was made between CA1 and the subiculum, leaving only a portion of the alveus intact[40]. The Schaffer collaterals were stimulated by placing a stimulation electrode between the two cuts in the stratum radiatum; the perforant

path was stimulated by an electrode placed between the two cuts in the stratum lacunosum moleculare, and the alveus was stimulated with an electrode placed in the alveus on the subiculum side of the cut through CA1 (refs. 40,41).

The disynaptic nature of IPSCs was confirmed either by its being completely abolished by NBQX (Fig. 5b) or by the lack of an effect of gabazine on the initial slope of the preceding EPSC (Fig. 6b).

### Cannabinoid sensitivity

We determined the cannabinoid sensitivity of recorded interneurons by depolarizing the postsynaptic pyramidal cell to 0 mV for 5 s (DSI) while stimulating action potentials in the connected presynaptic interneuron at 0.5 Hz. This protocol was repeated at least three times. Averages were made from five unitary IPSCs before depolarization, two after return to resting conditions, and five 1 min after recovery from depolarization (at least 15, 6 and 15 sweeps, respectively, were averaged, and are shown in the figures). Cannabinoid sensitivity in the majority of neurons were tested through DSI; however, in those few cases where interneurons had a very low probability of GABA release, cannabinoid sensitivity was assessed with the CB1R antagonist, AM-251 (ref. 42). We found four neurons whose unitary IPSCs were tonically suppressed and were revealed by the application of 5 μM AM-251; these cells were treated as CB1R-positive but were excluded from all quantifications in Figures 1 and 2.

### Paired recording statistics

We made 611 paired recordings from interneurons and pyramidal cells, of which 158 (25.9%) had inhibitory synaptic connections. Out of these 158, 85 were tested for cannabinoid sensitivity and 34 were cannabinoid sensitive. Of the cannabinoid-sensitive interneurons, 29 were identified as basket cells (of the remaining 5, one had a bistratified axonal arborization—this cell was not included in the study—and 4 could not be recovered). Of the 51 cannabinoid insensitive neurons, 26 were identified as basket cells (the remaining 25 interneurons were axo-axonic, bistratified, O-LM or unidentified). The first 16 DSI-sensitive and 11 DSI-insensitive basket cells collected in this study were reconstructed, and are described in Figure 2a and in Supplementary Figure 1.

### Analysis

Average values in the text and figures are expressed as mean ± s.e.m. We used the Student's *t*-test for statistical comparisons unless otherwise stated. All traces are the average of 10–20 sweeps, unless otherwise stated. Membrane time constants were measured by fitting a single exponential to the late portion of the membrane potential relaxation from a step current injection of −10 pA to −100 pA. Amplitudes were determined by finding the peak of an EPSC/IPSC as measured from a baseline before the stimulus artifact; if the EPSC/IPSC began before the decay of the previous stimulus, the decay was fit with a single exponential and the baseline extrapolated. The synaptic delay was measured from the peak of the action potential to the 10% rise of the IPSC. Jitter (Fig. 7) is defined as the standard deviation of the latency of the peak of the action potential.

### Morphology and immunocytochemistry

Slices were fixed in 4% paraformal-dehyde in 0.1 M phosphate buffer (PB), cryoprotected in a 30% sucrose PB solution, and then frozen in a methylbutane on dry ice. To recover biocytin-filled interneurons in whole-mount, slices were incubated overnight in 3% Triton, to allow full penetration of the ABC Kit (Vectastain). The neurons were revealed by a diaminobenzidine (DAB) reaction (0.5%) with nickel intensification (3% ammonium nickel

sulfate and 100 mM imidazole). Slices were dehydrated in ascending alcohols and xylenes and mounted in damar resin (Fluka). Interneuron soma, axons and dendrites were reconstructed on a light microscope at 40× using Neurolucida (MicroBrightField). We used Neuroex-plorer to quantify the length of the axonal and dendritic arborizations using 10 μm bins. To determine the colocalization of CB1R in recorded basket cell axons, we incubated the slices in 3% Triton and rabbit antibody to CB1R (1:1,000) overnight at room temperature. We then incubated the slices overnight at room temperature in 0.3% Triton, donkey anti-rabbit conjugated Alexa 594 (1:500) and streptavidin-conjugated Alexa 488 (1:1,000, Molecular Probes). Segments of biocytin-immunoreactive axons near the surface of the slice were selected randomly and confocal stacks (of 0.3 μm thickness) were taken in series with CB1R immunofluorescence at 60× (Olympus/Fluoview). Colocalization of biocytin and CB1R immunoreactivity was determined by inspection by a blind observer. Images shown in Figure 1 are the collapse of three 0.3 μm sections.

## Supplementary Material

Refer to Web version on PubMed Central for supplementary material.

## Acknowledgments

We thank P. Somogyi for his help in the morphological identification of basket cells and their discrimination from axo-axonic cells; C. Kapfer for his help in establishing immunohistochemical procedures; K. Mackie (University of Washington, Seattle) for his gift of the CB1R antibody; and J. Isaacson and the members of the Scanziani lab for comments on the manuscript. This work was funded by the US National Institutes of Health (MH71401, MH70058 and NIDA 5T32DA007315).

## References

1. Andersen P, Eccles JC, Loyning Y. Recurrent inhibition in the hippocampus with identification of the inhibitory cell and its synapses. Nature. 1963; 198:540–542. [PubMed: 14012800]
2. Mann EO, Suckling JM, Hajos N, Greenfield SA, Paulsen O. Perisomatic feedback inhibition underlies cholinergically induced fast network oscillations in the rat hippocampus *in vitro*. Neuron. 2005; 45:105–117. [PubMed: 15629706]
3. Cobb SR, Buhl EH, Halasy K, Paulsen O, Somogyi P. Synchronization of neuronal activity in hippocampus by individual GABAergic interneurons. Nature. 1995; 378:75–78. [PubMed: 7477292]
4. Miles R, Toth K, Gulyas AI, Hajos N, Freund TF. Differences between somatic and dendritic inhibition in the hippocampus. Neuron. 1996; 16:815–823. [PubMed: 8607999]
5. Pouille F, Scanziani M. Enforcement of temporal fidelity in pyramidal cells by somatic feed-forward inhibition. Science. 2001; 293:1159–1163. [PubMed: 11498596]
6. Fricker D, Miles R. EPSP amplification and the precision of spike timing in hippocampal neurons. Neuron. 2000; 28:559–569. [PubMed: 11144364]
7. Bartos M, et al. Fast synaptic inhibition promotes synchronized gamma oscillations in hippocampal interneuron networks. Proc Natl Acad Sci USA. 2002; 99:13222–13227. [PubMed: 12235359]
8. Freund TF. Interneuron diversity series: rhythm and mood in perisomatic inhibition. Trends Neurosci. 2003; 26:489–495. [PubMed: 12948660]
9. Bodor AL, et al. Endocannabinoid signaling in rat somatosensory cortex: laminar differences and involvement of specific interneuron types. J Neurosci. 2005; 25:6845–6856. [PubMed: 16033894]
10. Katona I, et al. Presynaptically located CB1 cannabinoid receptors regulate GABA release from axon terminals of specific hippocampal interneurons. J Neurosci. 1999; 19:4544–4558. [PubMed: 10341254]
11. Tsou K, Mackie K, Sanudo-Pena MC, Walker JM. Cannabinoid CB1 receptors are localized primarily on cholecystokinin-containing GABAergic interneurons in the rat hippocampal formation. Neuroscience. 1999; 93:969–975. [PubMed: 10473261]

12. Pitler TA, Alger BE. Depolarization-induced suppression of GABAergic inhibition in rat hippocampal pyramidal cells: G protein involvement in a presynaptic mechanism. Neuron. 1994; 13:1447–1455. [PubMed: 7993636]
13. Wilson RI, Nicoll RA. Endogenous cannabinoids mediate retrograde signalling at hippocampal synapses. Nature. 2001; 410:588–592. [PubMed: 11279497]
14. Nicoll RA, Alger BE. The brain's own marijuana. Sci Am. 2004; 291:68–75. [PubMed: 15597982]
15. Ali AB, Thomson AM. Facilitating pyramid to horizontal oriens-alveus interneurone inputs: dual intracellular recordings in slices of rat hippocampus. J Physiol (Lond). 1998; 507:185–199. [PubMed: 9490837]
16. Ali AB, Deuchars J, Pawelzik H, Thomson AM. CA1 pyramidal to basket and bistratified cell EPSPs: dual intracellular recordings in rat hippocampal slices. J Physiol (Lond). 1998; 507:201–217. [PubMed: 9490840]
17. McBain CJ, Fisahn A. Interneurons unbound. Nat Rev Neurosci. 2001; 2:11–23. [PubMed: 11253355]
18. Pouille F, Scanziani M. Routing of spike series by dynamic circuits in the hippocampus. Nature. 2004; 429:717–723. [PubMed: 15170216]
19. Losonczy A, Zhang L, Shigemoto R, Somogyi P, Nusser Z. Cell type dependence and variability in the short-term plasticity of EPSCs in identified mouse hippocampal interneurones. J Physiol (Lond). 2002; 542:193–210. [PubMed: 12096061]
20. Freund TF, Buzsaki G. Interneurons of the hippocampus. Hippocampus. 1996; 6:347–470. [PubMed: 8915675]
21. Klausberger T, et al. Brain-state- and cell-type-specific firing of hippocampal inter-neurons *in vivo*. Nature. 2003; 421:844–848. [PubMed: 12594513]
22. Klausberger T, et al. Complementary roles of cholecystokinin- and parvalbumin-expressing GABAergic neurons in hippocampal network oscillations. J Neurosci. 2005; 25:9782–9793. [PubMed: 16237182]
23. Hefft S, Jonas P. Asynchronous GABA release generates long-lasting inhibition at a hippocampal interneuron-principal neuron synapse. Nat Neurosci. 2005; 8:1319–1328. [PubMed: 16158066]
24. Deuchars J, Thomson AM. CA1 pyramid-pyramid connections in rat hippocampus *in vitro*: dual intracellular recordings with biocytin filling. Neuroscience. 1996; 74:1009–1018. [PubMed: 8895869]
25. Mittmann W, Koch U, Hausser M. Feed-forward inhibition shapes the spike output of cerebellar Purkinje cells. J Physiol (Lond). 2005; 563:369–378. [PubMed: 15613376]
26. Andersen P, Bland BH, Dudar JD. Organization of the hippocampal output. Exp Brain Res. 1973; 17:152–168. [PubMed: 4714522]
27. Wierenga CJ, Wadman WJ. Functional relation between interneuron input and population activity in the rat hippocampal cornu ammonis 1 area. Neuroscience. 2003; 118:1129–1139. [PubMed: 12732256]
28. Ameri A. The effects of cannabinoids on the brain. Prog Neurobiol. 1999; 58:315–348. [PubMed: 10368032]
29. Gulyas AI, Megias M, Emri Z, Freund TF. Total number and ratio of excitatory and inhibitory synapses converging onto single interneurons of different types in the CA1 area of the rat hippocampus. J Neurosci. 1999; 19:10082–10097. [PubMed: 10559416]
30. Matyas F, Freund TF, Gulyas AI. Convergence of excitatory and inhibitory inputs onto CCK-containing basket cells in the CA1 area of the rat hippocampus. Eur J Neurosci. 2004; 19:1243–1256. [PubMed: 15016082]
31. Faber DS, Korn H. Applicability of the coefficient of variation method for analyzing synaptic plasticity. Biophys J. 1991; 60:1288–1294. [PubMed: 1684726]
32. Sik A, Penttonen M, Ylinen A, Buzsaki G. Hippocampal CA1 interneurons: an *in vivo* intracellular labeling study. J Neurosci. 1995; 15:6651–6665. [PubMed: 7472426]
33. Katsumaru H, Kosaka T, Heizmann CW, Hama K. Immunocytochemical study of GABAergic neurons containing the calcium-binding protein parvalbumin in the rat hippocampus. Exp Brain Res. 1988; 72:347–362. [PubMed: 3066634]

34. Fukuda T, Aika Y, Heizmann CW, Kosaka T. Dense GABAergic input on somata of parvalbumin-immunoreactive GABAergic neurons in the hippocampus of the mouse. Neurosci Res. 1996; 26:181–194. [PubMed: 8953580]

35. Galarreta M, Erdelyi F, Szabo G, Hestrin S. Electrical coupling among irregular-spiking GABAergic interneurons expressing cannabinoid receptors. J Neurosci. 2004; 24:9770–9778. [PubMed: 15525762]

36. Andersen P, Eccles J. Inhibitory phasing of neuronal discharge. Nature. 1962; 196:645–647. [PubMed: 14012799]

37. Csicsvari J, Jamieson B, Wise KD, Buzsaki G. Mechanisms of gamma oscillations in the hippocampus of the behaving rat. Neuron. 2003; 37:311–322. [PubMed: 12546825]

38. Hajos N, et al. Cannabinoids inhibit hippocampal GABAergic transmission and network oscillations. Eur J Neurosci. 2000; 12:3239–3249. [PubMed: 10998107]

39. Morales M, Backman C. Coexistence of serotonin 3 (5–HT3) and CB1 cannabinoid receptors in interneurons of hippocampus and dentate gyrus. Hippocampus. 2002; 12:756–764. [PubMed: 12542227]

40. Dingledine R, Langmoen IA. Conductance changes and inhibitory actions of hippocampal recurrent IPSPs. Brain Res. 1980; 185:277–287. [PubMed: 7357430]

41. Alger BE, Nicoll RA. Feed-forward dendritic inhibition in rat hippocampal pyramidal cells studied *in vitro*. J Physiol (Lond). 1982; 328:105–123. [PubMed: 7131309]

42. Losonczy A, Biro AA, Nusser Z. Persistently active cannabinoid receptors mute a subpopulation of hippocampal interneurons. Proc Natl Acad Sci USA. 2004; 101:1362–1367. [PubMed: 14734812]

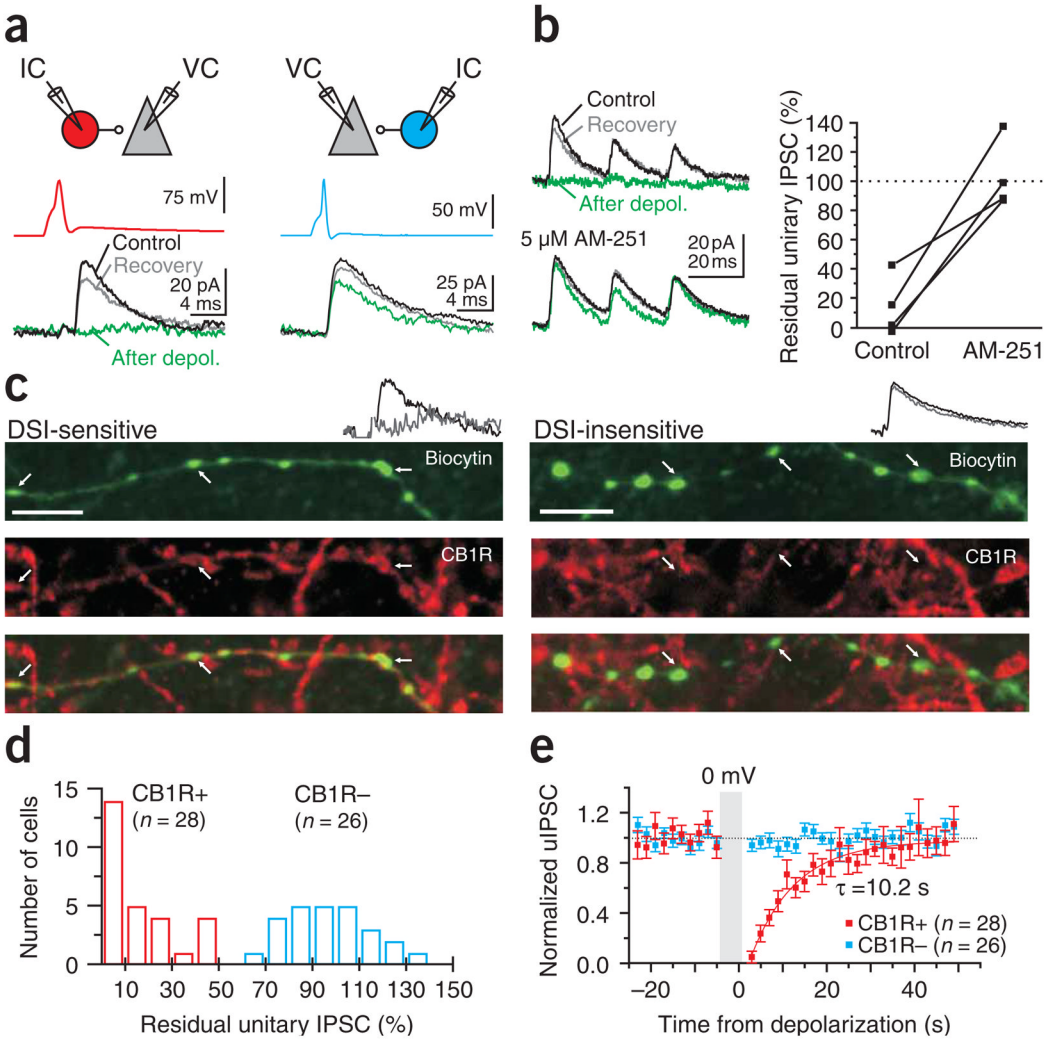


**Figure 1.**

Identification of CB1R-positive and -negative basket cells. (**a**) Top, schematic of the recording configuration. IC, current clamp; VC, voltage clamp. Bottom, current and voltage traces. Unitary IPSCs (uIPSCs) recorded in a pyramidal cell (black traces, $V_{holding}$ = −50 mV) in response to a spike triggered in a presynaptic basket cell (upper traces). Pyramidal cell depolarization (0 mV, 5 s) transiently suppressed the uIPSC (green traces) in some basket cells (left) but not in others (right). (**b**) Left, suppression of uIPSCs evoked by three action potentials at 50 Hz (upper traces) was abolished by the CB1R antagonist AM 251 (5 μM, lower traces). Right, summary graph ($n$ = 4). (**c**) Biocytin-filled axons (top), CB1R antibodies (middle) and their superposition (bottom) in DSI-sensitive (left) and -insensitive (right) basket cells. White arrows, boutons of the recorded interneuron. Scale bar, 5 μm. Note the colocalization of biocytin and CB1R in the DSI-sensitive basket cell. Inset (in all figures), current traces illustrating the presence or absence of DSI on the uIPSC in the recorded basket-to–pyramidal cell pair. Black trace, control. Gray trace, after depolarization. (**d**) Distribution of the uIPSC amplitudes after depolarization (54 pairs). Suppression, red bars ($n$ = 28). Lack of suppression, blue bars ($n$ = 26). The amplitude of the residual IPSC is the average of the uIPSCs collected 3 s and 5 s after the end of the depolarization (and hence shows a variable degree of recovery). (**e**) Summary (mean ± s.e.m.) of the time course of

uIPSCs suppression for CB1R-positive and -negative basket cells. Recovery is fitted with a single exponential.

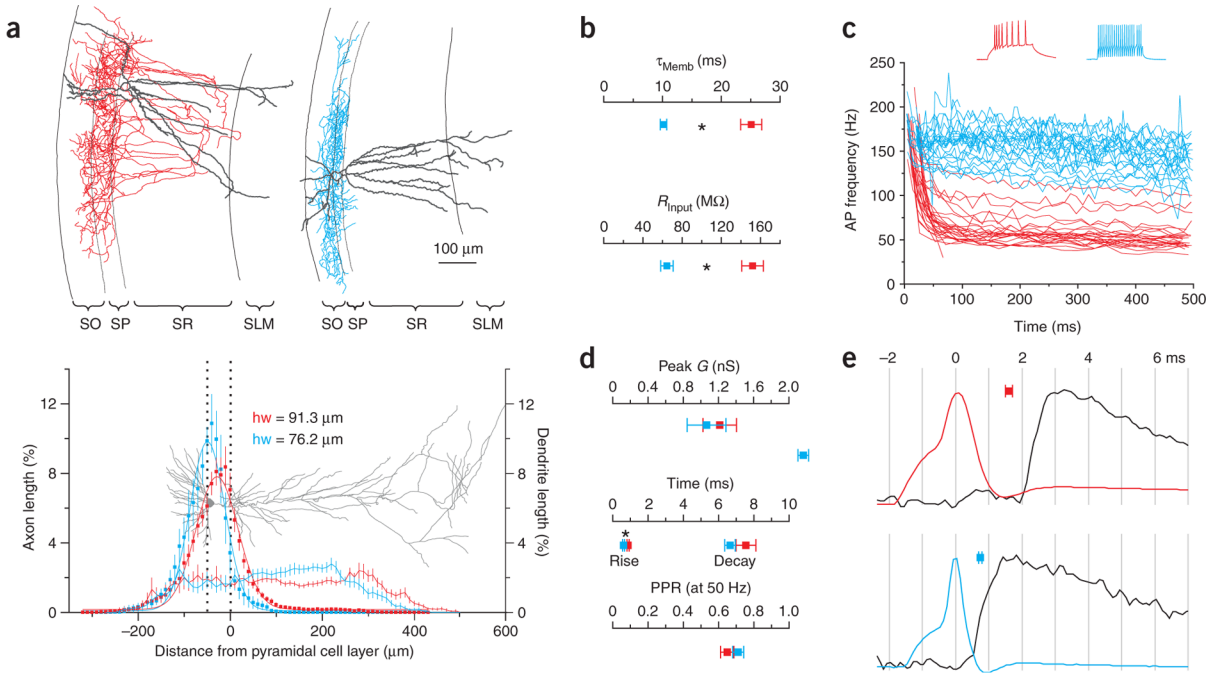


**Figure 2.**

Characterization of morphological, intrinsic and synaptic properties of CB1R-positive and -negative basket cells. (**a**) Top, reconstructions of CB1R-positive (left; red, axon; gray, dendrite) and -negative (right; blue, axon; gray, dendrite) basket cells shown in Figure 1a (all reconstructed cells are illustrated in Supplementary Fig. 1). SO, stratum oriens; SP, stratum pyrimidale; SR, stratum radiatum; SLM, stratum lacunosum-moleculare. Bottom, axonal (squares; $n = 16$ and 11) and dendritic (thin lines; $n = 13$ and 11; dotted lines represent SP; gray pyramidal cell for reference) density distributions of reconstructed basket cells. Axonal distributions are fit by Gaussians (thick lines; hw = half width). (**b**) Summary of membrane time constant (top) and input resistance (bottom) for CB1R-positive (red; $n =$ 18 and 22) and -negative (blue; $n = 22$ and 26) basket cells. Asterisks represent statistical significance ($P < 0.0001$). (**c**) Instantaneous spike frequency of CB1R-positive ($n = 28$) and CB1R-negative ($n = 26$) basket cells in response to depolarizing current pulses. Voltage traces from cells in **a**. (**d**) Summary graphs of peak conductance (top), rise time and decay time constant (middle), and paired pulse ratio (50 Hz, bottom) of uIPSCs evoked by CB1R-positive (red; $n = 28$, 26, 24 and 21) and -negative (blue; $n = 26$, 24, 23 and 12) basket cells. (**e**) Action potentials from cells in **a** and corresponding uIPSC in the postsynaptic pyramidal cell (black) on an expanded time scale (vertical lines are separated by 1 ms). Squares, average latencies (between action potential peak and uIPSC onset) for CB1R-positive (top, $n = 27$) and -negative (bottom, $n = 24$) basket cells.

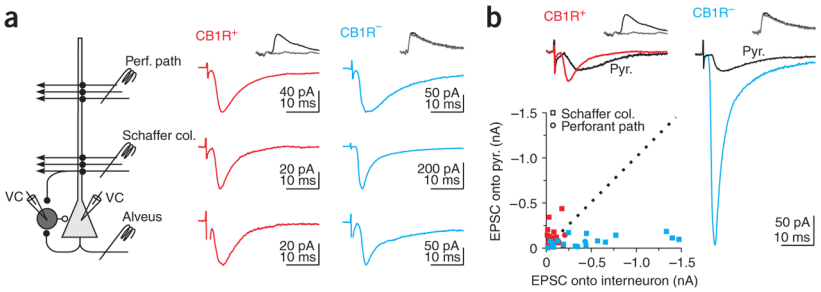


**Figure 3.**

Distinct excitation of CB1R-positive and -negative basket cells. (**a**) Left, schematic of recording configuration. Monosynaptic EPSCs recorded in a CB1R-positive (middle) and -negative (right) basket cell by stimulating three excitatory pathways. (**b**) Top, EPSC recorded simultaneously in connected basket-to–pyramidal cell pairs in response to Schaffer collaterals stimulation. Same cells as in **a**. In **a** and **b**, EPSCs were recorded in the presence of gabazine (2.5 μM) or at the IPSC reversal potential (−85 mV). Bottom, scatter plot of the amplitude of Schaffer collateral and perforant path EPSCs recorded in CB1R-positive (Schaffer collaterals, $n = 16$; Perforant path, $n = 7$) and -negative (Schaffer collaterals, $n = 16$; Perforant path, $n = 5$) versus their paired pyramidal cells. Dotted line, unity.

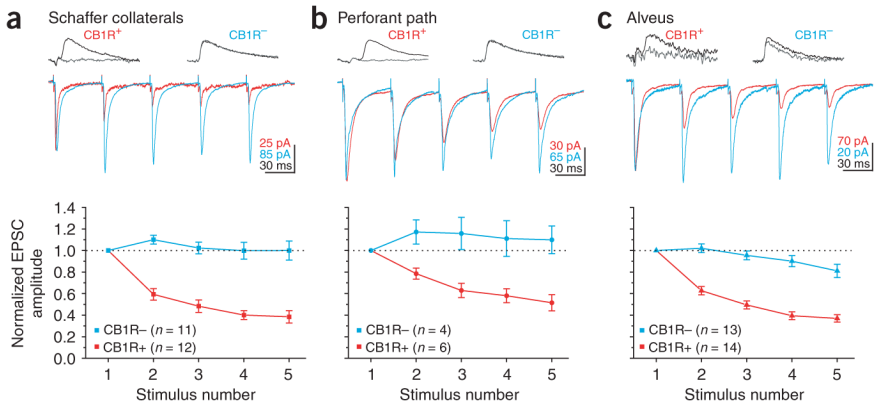


**Figure 4.**

Distinct dynamics of excitation of CB1R-positive and -negative basket cells. (**a**) Top, current traces in response to Schaffer collateral stimulation at 20 Hz in CB1R-positive and -negative basket cells (the traces have been scaled to the first EPSC). Bottom, summary graph of normalized EPSC amplitudes plotted against stimulus number. CB1R-negative cell is same as in Figure 3. All EPSCs in this figure were recorded in presence of gabazine (2.5 μM) or at the IPSC reversal potential (−85 mV). (**b**) Top, current traces in response to perforant path stimulation in CB1R-positive and -negative basket cells. Bottom, normalized EPSC amplitudes plotted against stimulus number. Both basket cells are the same as in Figure 3. (**c**) Top, current traces in response to alveus stimulation in CB1R-positive and -negative basket cells. Bottom, normalized EPSC amplitudes plotted against stimulus number.

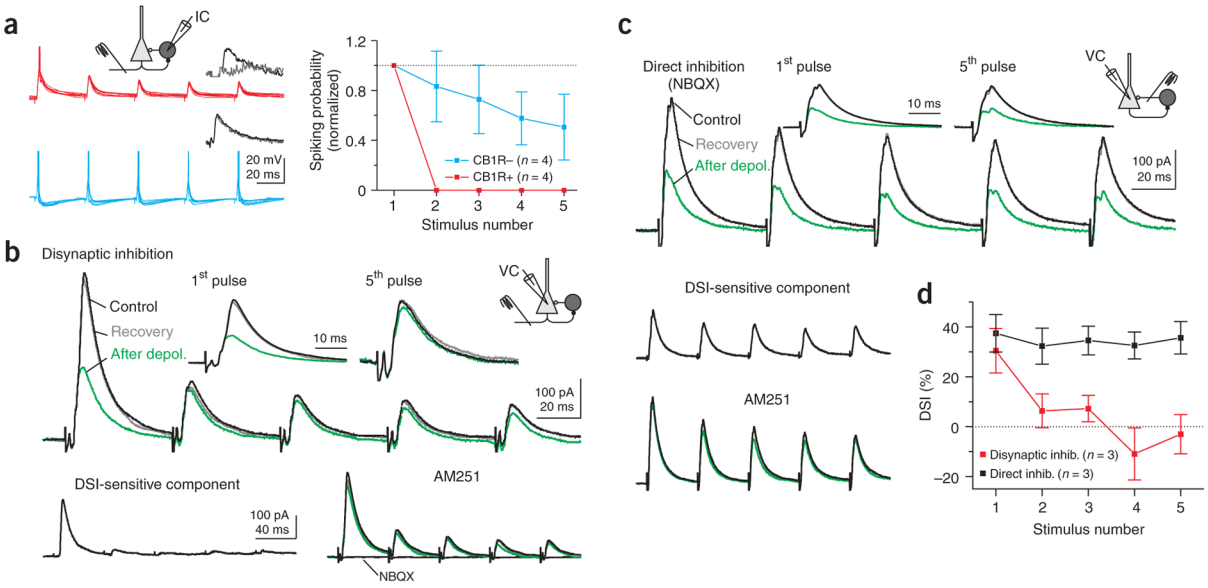


**Figure 5.**

Transient recruitment of CB1R-positive basket cells. (**a**) Left, ten superimposed voltage traces from CB1R-positive and -negative basket cells during 20 Hz alveus stimulation at threshold for spiking on the first stimulus. Action potentials have been truncated. CB1R-positive cell is the same as that shown in Figure 1c. Right, spiking probability plotted for each stimulus in the train, normalized to the probability of spiking in response to the first stimulus in CB1R-positive and -negative basket cells. (**b**) Upper traces, disynaptic IPSCs recorded in a pyramidal cell in response to repetitive alveus stimulation (five stimuli at 20 Hz) before (black), directly after (green) and upon recovery from (gray) depolarization (0 mV, 5 s). Insets, first and fifth responses scaled. Lower traces, the DSI-sensitive component was isolated by subtracting the green from the black trace (top panel). Right, the CB1R antagonist AM251 (5 μM) blocked suppression of the IPSC. The glutamate receptor antagonist NBQX (10 μM) abolished the IPSCs, confirming their disynaptic nature. (**c**) Upper traces, monosynaptic IPSCs (five stimuli at 20 Hz) in the presence of NBQX with the stimulation electrode placed near the pyramidal cell body. Lower traces, the DSI-sensitive component was isolated as in **b**, and the CB1R antagonist blocked suppression of the IPSC. (**d**) DSI plotted against stimulus number for monosynaptic (black) and disynaptic (red) IPSCs.

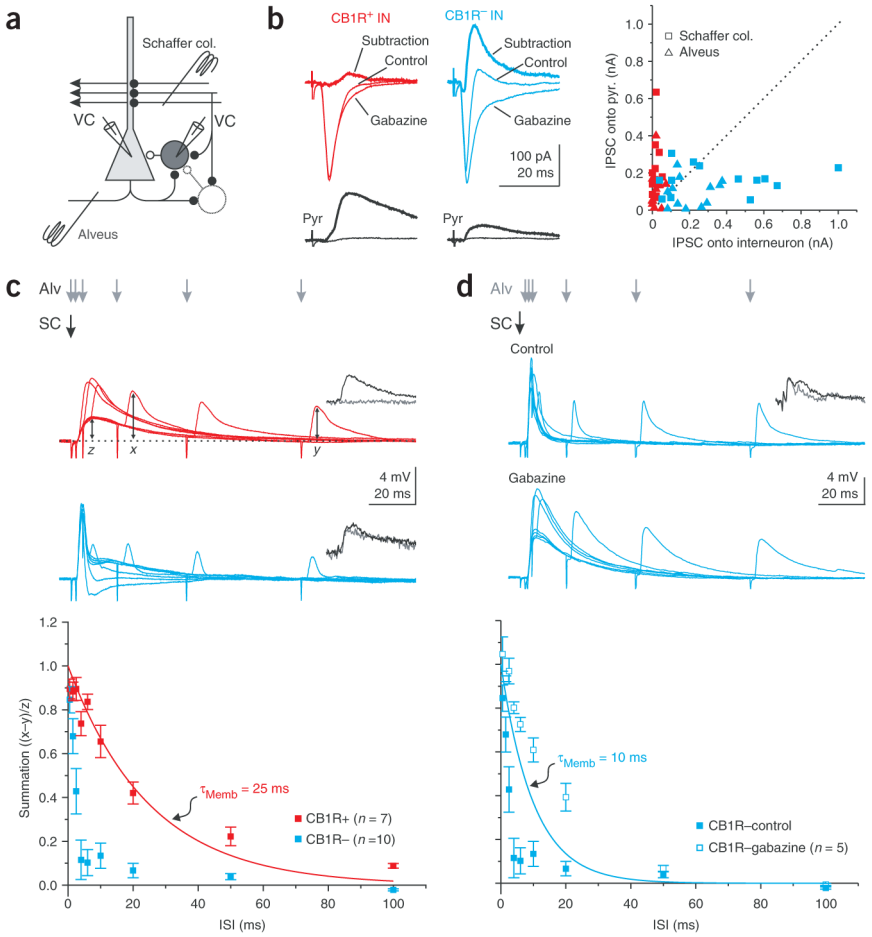


**Figure 6.**

Distinct integration time windows in CB1R-positive and -negative basket cells. (**a**) Recording configuration. (**b**) Left, current traces from CB1R-positive and -negative basket (top) and pyramidal cell (bottom) pairs in response to alveus stimulation in control and gabazine, and the algebraic subtraction of the traces (thick line). CB1R-positive cell is the same as that in Figure 1b. Right, scatter plot of IPSCs onto paired basket and pyramidal cells elicited by Schaffer collateral ($n$ = 11 and 13 for CB1R-positive and -negative basket cells, respectively) and alveus ($n$ = 12 for both CB1R-positive and -negative basket cells) stimulation. (**c**) Top, superimposed average voltage traces from basket cells in response to Schaffer collateral stimulation (black arrow) followed, with increasing delays, by alveus stimulation (gray arrows). Data from same cells as those in **b**. Bottom, summation is computed as the peak amplitude of the summed response ($x$) minus the peak amplitude of the feedback postsynaptic potential (PSP) alone ($y$), normalized by the peak of the feedforward PSP ($z$). The result is plotted against the interstimulus interval (ISI) for CB1R-positive and -negative basket cells. Red line, membrane time constant of CB1R-positive basket cells. (**d**) Top, superimposed average voltage traces from a CB1R-negative basket cell in control and in the presence of gabazine for the same protocol as in **c**. Bottom, summation is plotted against the ISI in control (same data as in **c**) and in gabazine. Blue line, membrane time constant of CB1R-negative basket cells.

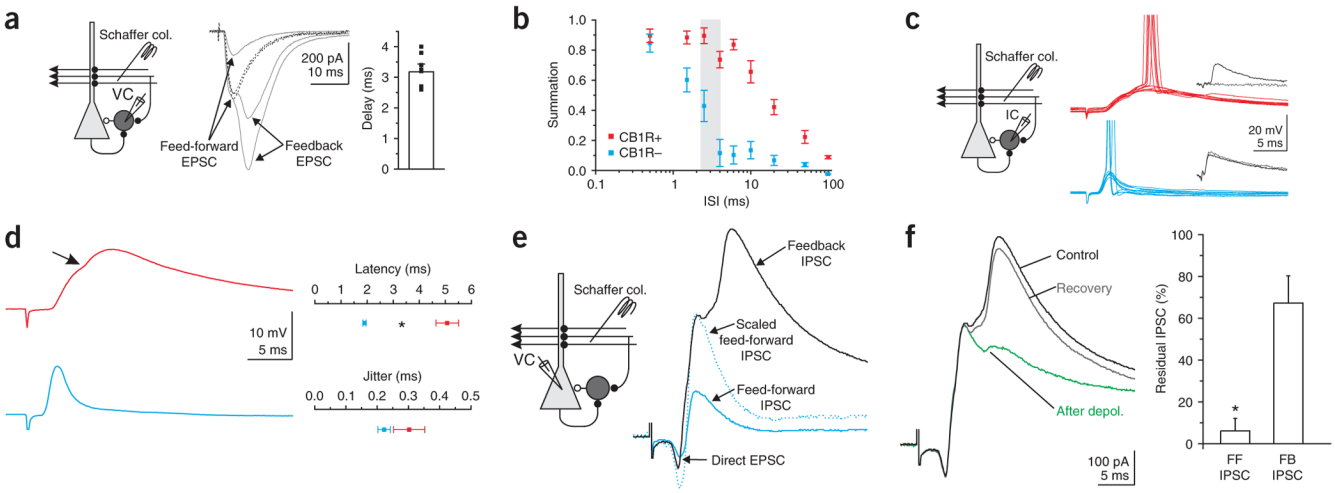


**Figure 7.**

Differential contribution of CB1R-positive and -negative basket cells to feed-forward and feedback inhibition. (**a**) Left, recording configuration. Center, voltage-clamp recording from an interneuron in response to Schaffer collateral stimulation at three different intensities (2.5 μM gabazine). Note the appearance of a late, feedback EPSC at stronger stimulation intensities. Dotted trace, the EPSC recorded at low stimulus intensity is scaled to the peak of the early component elicited at strong stimulation intensities. Right, delays between feedforward and feedback EPSCs ($n = 7$). (**b**) Same data as in Figure 6c plotted on a logarithmic axis. The vertical gray shaded region represents the range of delays recorded in **a**. (**c**) Left, recording configuration. Right, ten superimposed current traces from CB1R-positive (top, red) and -negative (bottom, blue) basket cells at threshold for spiking in response to Schaffer collateral stimulation. Action potentials have been truncated. (**d**) Left, average of responses that did not elicit an action potential (same cells as in **c**). Note the discontinuity (arrow) in the rise of the EPSP in the CB1R-positive cell, due to the onset of the feedback EPSP. Right, summary of latency to spike and jitter in CB1R-positive ($n = 4$) and -negative ($n = 9$) basket cells. (**e**) Left, recording configuration. Right, voltage-clamp recording from a pyramidal cell in response to Schaffer collateral stimulation at two different intensities (blue trace, low intensity; black trace, high intensity). Note the appearance of a late, feedback IPSC at the stronger stimulation intensity. Dotted trace, the feedforward IPSC elicited at low stimulation intensity scaled to the peak of the feedforward IPSC elicited at high intensity. (**f**) Feedforward and feedback IPSCs before (black), directly after (green) and on recovery from (gray) depolarization. Right, summary of suppression of the feedforward and feedback IPSCs ($n = 5$).

**Table 1**

Ratio of the fifth to the first EPSC evoked by stimulating the three main afferents with trains of five stimuli

| | 10 Hz (stim5/stim1) | | 20 Hz (stim5/stim1) | | 50 Hz (stim5/stim1) | |
|---|---|---|---|---|---|---|
| **Pathway** | **CB1R$^+$** | **CB1R$^-$** | **CB1R$^+$** | **CB1R$^-$** | **CB1R$^+$** | **CB1R$^-$** |
| Schaffer col. | 0.49 ± 0.04 (17) | 0.99 ± 0.05 (15)* | 0.38 ± 0.06 (12) | 1.00 ± 0.09 (11)* | 0.25 ± 0.04 (11) | 0.96 ± 0.13 (10)* |
| Alveus | 0.48 ± 0.03 (19) | 0.86 ± 0.06 (17)* | 0.37 ± 0.03 (14) | 0.81 ± 0.06 (13)* | 0.30 ± 0.04 (14) | 0.68 ± 0.08 (12)* |
| Perf. path | 0.60 ± 0.07 (7) | 1.18 ± 0.16 (4)* | 0.52 ± 0.08 (6) | 1.10 ± 0.13 (4)* | 0.38 ± 0.07 (6) | 0.93 ± 0.10 (4)* |

Note the larger depression on CB1R positive as compared to negative basket cells. The number of cells is given in parentheses; significant differences ($P < 0.05$) between CB1R positive and negative basket cells are indicated with an asterisk.